A New Boundary Element Method for Multiple-Frequency Parameter Extraction of Lossy Substrates

Xiren Wang, Wenjian Yu, Zeyi Wang

Department of Computer Science and Technology,
Tsinghua University, Beijing 100084, China
Tel: 86-10-6277-3440, Fax: 86-10-6278-1489, e-mail: yu-wj@tsinghua.edu.cn

Abstract - The couplings via realistic lossy substrates can be modeled as frequency-dependent coupling parameters. The fast extraction at multiple frequencies can be accomplished in two sequent steps. The first is to extract the coupling resistance using a direct boundary element method (DBEM). The second is to revise the resistance into the parameter at the frequency in an exact and rapid way. The first step is time-consuming, while it runs only one time; the second repeats at each frequency, but is much easier. For more frequency calculation, this method is more advanced. Numerical experiments illustrate that this method has high accuracy, and it can be hundreds of times faster than an advanced Green's function based method. Substrates with arbitrary doping profiles can also be easily handled, which is partly verified by experiment.

I Introduction

There are currently increasing demands for high-integration [1]. Digital and analog components are often built on a single substrate. Such high-integration circuits have some advantages, such as low cost [2]. However, the coupling noises traveling through the shared substrate will bring some challenges for designs. One reason of the coupling is that digital components will inject current noises into the substrate. Since the substrate is not a perfect insulator, the noises travel throughout the substrate, and severely impact some others, such as sensitive analog components [3]. In addition, the substrate coupling also impacts other circuit performances. For example, the quality factor of inductors is important for wireless communication circuits. However, the factor is limited by substrate losses, especially at high frequencies. In a word, the acknowledge of lossy substrates is necessary even critical for designs [4].

At low frequencies up to several gigahertz, a resistive model is efficient to model substrate couplings. Numerical methods for the resistance extraction include finite element method (FEM), finite difference method (FDM) [5], and methods based on Green's function (sometimes also called boundary element method) [2, 4, 6, 7]. The efficiency of FEM and FDM is not high, since they discretize entire volume of substrates. However, they can handle substrates with arbitrary doping profiles.

The Green's function based methods [2, 6, 7] are generally more efficient, since they only discretize contact surfaces. A Green's function that satisfies correlative boundary conditions (including continuity condition among different medium interfaces) needs to be found, which usually consists of multiple infinite series for multilayered substrates. The function generally consumes considerable computation. Accelerations may include the discrete cosine transform (DCT) [7] and eigendecomposition ideas. Anyway, these methods are limited to stratified substrates.

At high frequencies, the frequency-dependent parameter is desired for coupling model. The above Green's function based methods except that in [4] can not calculate the parameter easily. Unfortunately, the method in [4] was not always stable [8]. In reality, its program ASITIC [9] may run very slowly, which is obvious in our numerical experiments. Moreover, it is also limited to layered substrates.

In reality, substrates are not always stratified. There are lots of such non-stratified substrates, such as oxide wells, trenches, sinkers, buried diffusions and etc [10]. There are special structures like Faraday shields and junction shields [11] for noise reduction. To simulate these substrates, the methods based on Green's function meet much difficulty. FEM and FDM have no theoretic difficulty, but their application is not practical.

For comprehensive evaluation of the substrate coupling, the parameter values at multiple frequencies are desired. In this paper, the direct boundary element method (DBEM) [12, 13] is improved for efficient extraction of the parameters. DBEM is used to get the substrate resistance [12]. This is performed only one time. Then, according to mathematical formulas, the resistance is transformed equally into the desired parameter at any frequency. However, the transformation is much easier. Numerical experiments illustrate that the proposed approach is highly efficient for multiple-frequency calculation. For a complicated substrate, it is hundreds of times faster than the advanced ASITIC [9], as well as of high accuracy. On the other hand, only the free-space Green's function is used, and then the method is capable to simulate much more complicated than layered substrates, which is also illustrated by experiment.

The rest texts are organized as follows. Section 2 will give the DBEM principle for resistance extraction, and the high-frequency parameter extraction. The next section will illustrate how to revise resistance into high-frequency parameter. Section 4 will include numerical experiments to show the accuracy and efficiency of the presented revising method. A non-stratified substrate is simulated, showing the good versatility of DBEM. The last is conclusions.

This work is supported by National Natural Science Foundation of China under Grant 60401010.

1-4244-0630-7/07/$20.00 ©2007 IEEE.

II. Resistance and High-Frequency Parameter Extraction Using DBEM

Fig. 1 is an example of a lossy substrate, consisting of three layers of mediums M_1, M_2 and M_3. As usual, there is a grounded plane on the bottom. There are some contacts C_j, which are the windows communicating with outside circuits. In many literatures, contacts are assumed to be only on the top, and of zero height. Here, however, they can lie anywhere necessarily, and can have their own heights.

A. Resistance extraction using DBEM

At low frequency (up to several gigahertz), the resistive coupling is dominate. The resistance can be obtained through setting bias voltages on contacts and then calculating current flows. Assume no current flows through the boundary except for contacts, producing the following conditions:

$$u = \overline{u}\text{, on contact surfaces} \tag{1a}$$

$$E_n = 0\text{, on natural boundary} \tag{1b}$$

where E_n is the normal field intensity. Within each medium in the substrate, the potential u satisfies the Laplace equation:

$$\nabla^2 u = 0. \qquad \text{in medium } M_i \tag{2}$$

The potential and the conductance current are continuous across medium interfaces:

$$u_a = u_b, \tag{3a}$$

$$\sigma_a E_{n,a} = \sigma_b E_{n,b}, \tag{3b}$$

where σ_a (σ_b) is the conductivity of medium a (b).

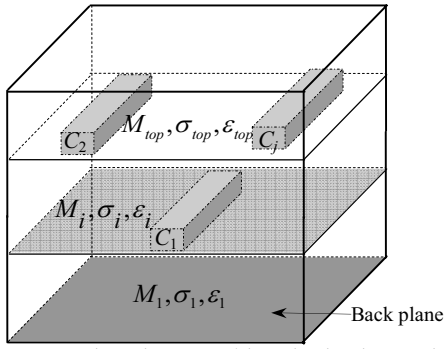

Fig. 1. An example substrate with a back plane. The non-zero conductivity of medium M_i is σ_i, and the permittivity is ε_i.

Equation (2) can be transformed into a boundary integral equation (BIE) [12] defined on the boundary of medium M_i. Partition the boundary into N_i elements Γ_{ij}, resulting [11]:

$$c_s u_s + \sum_{j=1}^{N_i} \int_{\Gamma_{ij}} q^* u d\Gamma = \sum_{j=1}^{N_i} \int_{\Gamma_{ij}} u^* E_n d\Gamma, \text{ for } M_i \tag{4}$$

where collocation point s is on one boundary element of M_i. c_s is 0.5 for smooth surfaces. u^* is the fundamental solution of Laplace equation, or the free-space Green's function $1/(4\pi r)$, where r is the distance between point s and a source point [12]. q^* is the normal derivative.

Here, assume u (or E_n) on an element is constant. The coefficient of them is in $\int_{\Gamma_{ij}} q^* d\Gamma$ (or $\int_{\Gamma_{ij}} u^* d\Gamma$) form.

List the equations (4) for each medium in the substrate. Combine these equations with the interface conditions (3). Substitute the conditions (1), and we get an overall system

$$A_{res} X_{res} = B. \tag{5}$$

Solving the system. The resistance can be obtained:

$$R_{mk} = \frac{1}{\int_{\Gamma_k} \sigma E_n d\Gamma} \tag{6}$$

where Γ_k is the surface of contact k, and σ is the conductivity (reciprocal of resistivity) of the medium around contact k.

B. High frequency parameter extraction using DBEM [13]

The resistance model is efficient only at low frequencies. At high frequency, the full current, other than conductance current, is continuous across interfaces:

$$(\sigma_a + j\omega\varepsilon_a) E_{n,a} = (\sigma_b + j\omega\varepsilon_b) E_{n,b}, \tag{7}$$

where ε is the medium permittivity, and ω is the angular frequency.

Replace the (3b) with (7), remain (1), (3a), and (4) unchanged, and we can get a linear system:

$$A X = B \tag{8}$$

Note that this matrix B is equal to that in (5), because they are both merely related to preset voltages and spatial integrals in $\int_{\Gamma_{ij}} q^* d\Gamma$ form. The coupling parameter is:

$$Z_{mk} = \frac{1}{\int_{\Gamma_k} (\sigma + j\omega\varepsilon) E_n d\Gamma}. \tag{9}$$

Obviously, Z_{mk} depends on the frequency. The parameters at many frequencies are necessary for the comprehensive knowledge about the coupling. A trivial calculation is to build and solve (8) repeatedly, while the efficiency decreases considerably with the frequency point number.

III. High-Frequency Parameter Extraction via Resistance

The high-frequency parameter at multiple frequency points can be obtained indirectly. At first, coupling resistance can be obtained through (1) ~ (5); and then the resistance is modified into the desired high-frequency parameter.

A. Basic principle

There are close relations between the matrix A in (8) and A_{res} in (5). Take a look at how A_{res} is built. List the equations (4) for all the mediums in the substrate. The coefficient of a

non-interface variable of type E_n on medium M_1 is $\int_{\Gamma_{1e}} u^* d\Gamma$, where Γ_{1e} is an element on the boundary of M_1. Similarly, the coefficient of a variable of type u is $\int_{\Gamma_{1e}} q^* d\Gamma$.

Then combine these equations into an overall system using conditions (3a) and (3b). Take Γ_{12}, the interface element between mediums M_1 and M_2, as an example. There are two variables on Γ_{12}, denoted by u_{12} and q_{21} respectively. Assume that the coefficient of q_{21} corresponding to collocation points in M_2 is the integral over an element Γ_{2e} on M_2, i.e. $\int_{\Gamma_{2e}} u^* d\Gamma$ form. List (4) for M_1, where the coefficient of q_{21} corresponding to collocation points in M_1 is $\int_{\Gamma_{1e}} u^* d\Gamma$ (element Γ_{1e} is on M_1) multiplied by $r_{12}=\frac{\sigma_2}{\sigma_1}$, according to (3b).

A schematic diagram is shown in Fig. 2. $\mathbf{S_{21}}$, the coefficient of variable q_{12} for collocation points in M_2, comes from the spatial integral $\int_{\Gamma_{2e}} u^* d\Gamma$. And the coefficient of q_{12} for collocation points in M_1 is $\mathbf{S_{12}}$ (in $\int_{\Gamma_{1e}} u^* d\Gamma$ form) multiplied by $r_{12}=\frac{\sigma_2}{\sigma_1}$. The similar is true for $\mathbf{S_{32}}$ and $r_{23}\mathbf{S_{23}}$.

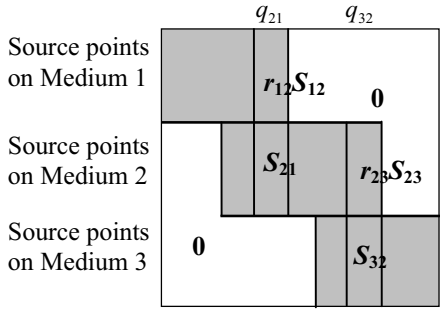

Fig. 2. Schematic diagram of the matrix A_{res} in (6) for the example substrate in Fig.1. Only the grey blocks are non-zeros. All the entries are real numbers.

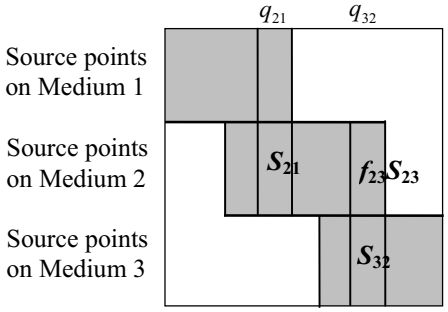

Fig. 3. The matrix A in (8) for high-frequency extraction. The entries marked with $f_{12}S_{12}$ and $f_{23}S_{23}$ are complex, and depend on the frequency.

Analogously, the diagram of the matrix A is in Fig. 3, where $f_{12}=\frac{\sigma_2+j\omega\varepsilon_2}{\sigma_1+j\omega\varepsilon_1}$, $f_{23}=\frac{\sigma_3+j\omega\varepsilon_3}{\sigma_2+j\omega\varepsilon_2}$ (refer to (7)).

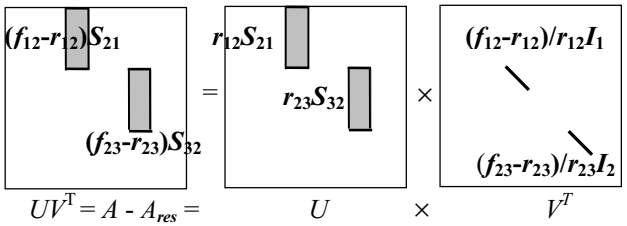

Fig. 4. Matrix $A - A_{res}$. U is a part of A_{res}. V consists of diagonal sub-matrices $(f_{12}/r_{12}-1)I_1$ and $(f_{23}/r_{23}-1)I_2$, where I_1 and I_2 are unit matrices.

If we let $f_{12}=r_{12}$, $f_{23}=r_{23}$, matrix A turns into A_{res}. This demonstrates the high similarity between them, while their difference is with lots of zero entries, as shown in Fig. 4.

Furthermore, the difference matrix can be decomposed into UV^T form, which is concluded by:

Theorem 1:

Matrices A in (8) and A_{res} in (5) are related by $A=A_{res}+UV^T$, where U and V are sparse matrices, and U is a subset of A_{res}.

Refer to Sherman-Morrison-Woodbury formula [14] $(A+UV^T)^{-1} = A^{-1} - A^{-1}U(I+V^TA^{-1}U)^{-1}V^TA^{-1}$, obtaining:

Theorem 2:

The solution of (8) $A^{-1}B$ can be obtained through $A_{res}^{-1}B$, which is the solution of (5).

Proof:

According to Theorem 1 and the above formula,

$$X = A^{-1}B = (A_{res} + UV^T)^{-1}B$$
$$= A_{res}^{-1}B - A_{res}^{-1}U(I+V^TA_{res}^{-1}U)^{-1}V^TA_{res}^{-1}B$$
$$= X_{res} - A_{res}^{-1}U(I+V^TA_{res}^{-1}U)^{-1}V^TX_{res}. \quad (10)$$

Therefore, solving (8) can be accomplished through X_{res}. In other words, the high-frequency parameter is obtained by revising the resistance. Since both X_{res} and $A_{res}^{-1}U$ are frequency-independent, they can be calculated and saved during extracting the resistance. At each frequency, they are loaded and modified using $(I+V^TA_{res}^{-1}U)^{-1}$. However, it is usually not easy to get the latter large complex matrix. For better efficiency, its special structure can be utilized.

B. Efficient implementation

Theorem 3:

Getting the $(I+V^TA_{res}^{-1}U)^{-1}$ in (10) equals to inversing its compressed form M, whose size is the total number of variables on the interfaces between 'different' mediums. 'Different' here means the conductivity or permittivity of the interfacing counterparts is not equal to each other.

Proof:

Since most entries of V^T and U are zero, $I+V^TA_{res}^{-1}U$ and $(I+V^TA_{res}^{-1}U)^{-1}$ are very similar to unit matrices. See Fig. 5 for example. M consists of the non-zero blocks in $I+V^TA_{res}^{-1}U$. Calculate $W=M^{-1}$, and re-fill the blocks into a unit matrix as large as $I+V^TA_{res}^{-1}U$, and then we get the

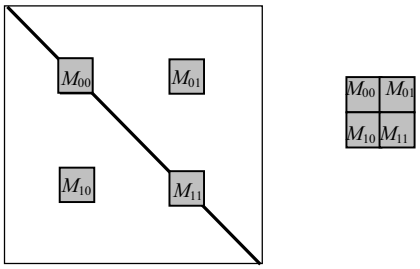

Fig. 5. Matrix $I+V^{\mathrm{T}}A_{res}^{-1}U$ and its compressed form *M*.

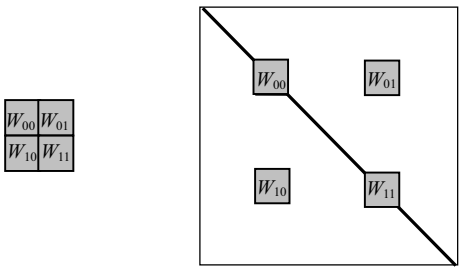

Fig. 6. The inversion of *M* (left). Re-fill $W=M^{1}$ into a large unit matrix (right). And thus $(I+V^{\mathrm{T}}A_{res}^{-1}U)^{-1}$ is obtained.

$(I+V^{T}A_{res}^{-1}U)^{-1}$. This processing can be expressed as:

$$I+V^{T}A_{res}^{-1}U \rightarrow M \rightarrow W = M^{-1} \rightarrow (I+V^{T}A_{res}^{-1}U)^{-1} \quad (11)$$

The equality of (11) can be easily verified in theory.

The size of *M* is exactly the total number of the variables on the interfaces between 'different' mediums. Refer to the entry values of matrix *V*. For interfaces between 'different' M_1 and M_2, the factor $(f_{12}/r_{12}\text{-}1)I_1$ is certainly not zero, because f_{12} varies with frequency. However, if M_1 and M_2 have the same conductivity and permittivity, this factor is certainly zero, due to $r_{12}=\dfrac{\sigma_2}{\sigma_1}=1=\dfrac{\sigma_2+j\omega\varepsilon_2}{\sigma_1+j\omega\varepsilon_1}=f_{12}$. Therefore, only for 'different' mediums, the corresponding entries in V^T are not zero, and so are blocks in $I+V^{T}A_{res}^{-1}U$. Thus, the exact size of matrix *M* is proven.

C. Algorithm flow

1. Generate A_{res} in (5). Select some entries to form *U*;
2. Solve for $X_{res}=A_{res}^{-1}B$ as well as for $A_{res}^{-1}U$;
3. For each frequency point, calculate the corresponding *Z*:
   a) Create such factors as $(f_{12}/r_{12}\text{-}1)I_1$ and $(f_{23}/r_{23}\text{-}1)I_2$, so as to form matrix *V*;
   b) Compress $I+V^{T}A_{res}^{-1}U$ into small matrix *M*;
   c) Inverse matrix *M*, and get *W*;
   d) Refill *W* to get matrix $(I+V^{T}A_{res}^{-1}U)^{-1}$;
   e) Get $X=X_{res}-A_{res}^{-1}U(I+V^{T}A_{res}^{-1}U)^{-1}V^{T}X_{res}$.
   f) Get the desired *Z* parameter through (9).

The above algorithm is very efficient and accurate, since it is strictly based on the Woodbury formula.

In (10), only X_{res} and non-zero blocks of $A_{res}^{-1}U$, $I+V^{T}A_{res}^{-1}U$ and $(I+V^{T}A_{res}^{-1}U)^{-1}$ need memory, but these blocks are small. Therefore, the memory usage excluding that used in calculating X_{res} is limited.

IV. Numerical Results

The first experiment is a substrate involving a top contact and a back plane, as shown in Fig. 7. The test case will be configured with two types of substrate processes [4], as shown in Fig. 8. In order to be compatible with literature data, the contacts are assumed to be of zero heights.

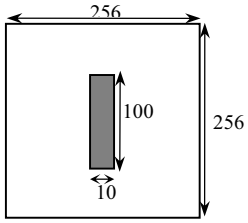

Fig. 7. A single contact at center (top view).

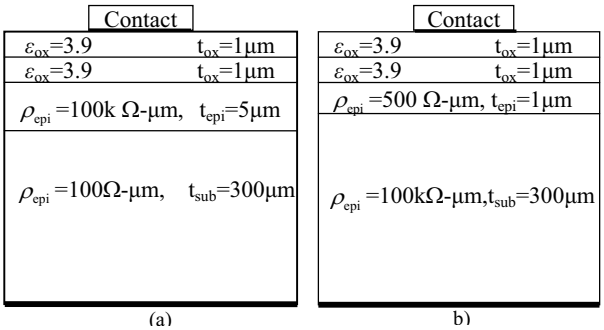

Fig. 8. Side views of two doping profiles [4]. (a) Low-resistivity (LR) process; b) high-resistivity (HR) process. Bottom bold lines denote back planes.

For the first test case, the coupling parameters obtained with the presented DBEM are depicted in Fig. 9 (for the LR process). The data in [4] are also depicted. The parameter when configured with the HR process is very similar to those in Fig. 9, here omitted. The figure indicates that with any process, the magnitude decreases as the frequency increases. This is because the substrate current injection is capacitive in nature [4]. The parameter is smaller in magnitude with the LR process than with the HR process. This is because the bulk is with much smaller resistivity in the LR process.

Both the magnitude and the phase of the coupling paramters obtained with DBEM are very close to literature data. The discrepancy is within 1.0%. In a word, DBEM has high accuracy.

To examine the efficiency, run DBEM and ASITIC [9] which is based on the algorithms in [4] on the same workstation. For a typical 52-contact substrate [2], the parameter comparison is listed in Table 1.

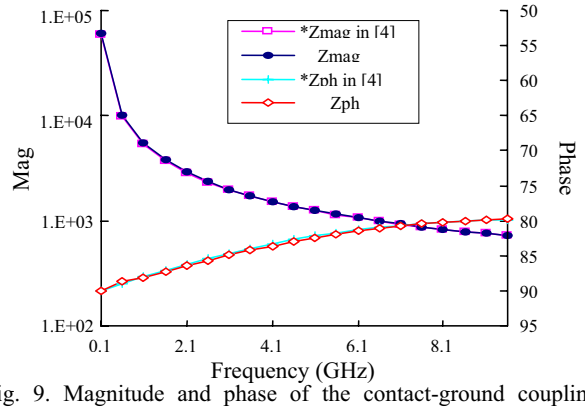

Fig. 9. Magnitude and phase of the contact-ground coupling parameters of the single-contact substrate with the LR process.

TABLE 1
DBEM vs. ASITIC for a Complicated Case with HR Process

Program	DBEM	ASITIC[9]		
#Contacts	52	52		
#Variables	7252	483	860	4352 (default)
PreCal Time (s)	420.9	360	360	360
Memory (MB)	60	24	32	310
Time (s.)	9.0	1930	9000	Not Obtained

"PreCal time" of DBEM is the time cost to calculate the resistance, which is performed only once. While that of ASITIC is the time to get the Green's function and its DCT.

There are as many as 7252 elements in DBEM, but it only takes DBEM 9.0 seconds to calculate the coupling parameters at a specified frequency. The higher efficiency is mainly brought by the small matrix M (size 587x587) in (11). As for ASITIC, the preparing time is comparable to DBEM, but the extraction time is much larger, even with a quite simplified mesh. Obviously, the performance of ASITIC with the default mesh will be more unacceptable. Besides, the memory usage of DBEM is much less than ASITIC.

The doping profiles in Fig. 8 are both stratified. However, for substrates with non-stratified doping profiles, the methods based on Green's function have much difficulty in handling them. In reality, there are many such substrates. For example, there are many lateral variation components in the substrates, such as oxide trenches and wells [9].

However, DBEM has enough versatility coving such non-stratified substrates, as shown in Fig. 10, where the top central block in gray has a distinct resistivity from its lateral neighbor. We call the block "LVB" (lateral variation block). Changing the dimension of the higher-resistivity LVB block will have impact on the contact-contact coupling parameters. The parameters obtained with DBEM are depicted in Fig. 11.

The figure illustrates that when the LVB block is small (L=0, or L=20), the coupling parameter is relatively small. As the block grows large (L=70), the parameter increases, since it obstructs the ohmic current flow remarkably. For a specified frequency, the difference between the parameters is small. A reason is that the obstructing LVB block can not be very large due to spatial limitation. Then, it is clear that DBEM is able to simulate such complex substrates without any difficulty.

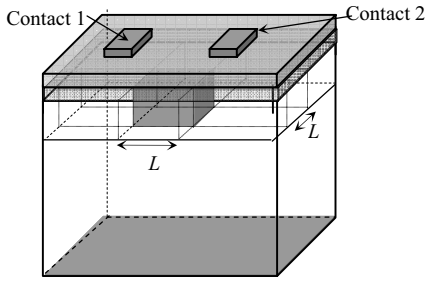

Fig. 10. Substrate with lateral resistivity variation in the epi layer based on the HR process. The width and length of the substrate are 200 μm. The resistivity of the epi layer and the gray block are 5e-4 and 0.5 Ωm, repectively. Note that each contact here is modeled as a block with 3-D shape, as well as the LVB block.

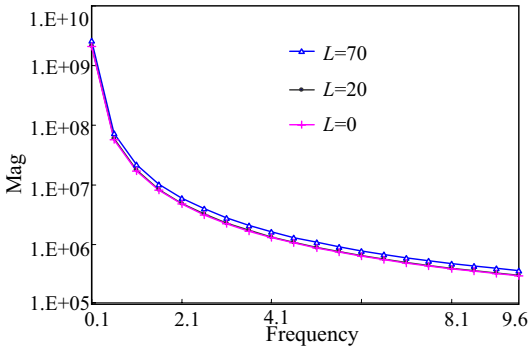

Fig. 11. Magnitudes of the contact-contact coupling parameters. Since the epi layer of HR process is very small, the central block is not possible to be large, and thus the curves are close to each other.

V. Conclusion

An efficient direct boundary element method (DBEM) is proposed to extract the high-frequency parameters of lossy substrates. Firstly, the coupling resistance of the substrates is obtained. Secondly, the resistance can be efficiently revised into the parameter at any frequency. The revising algorithm is strictly based on a mathematical formula, and no accuracy is sacrificed in the revising. Numerical experiments indicate that DBEM can have a high accuracy, and it can be hundreds of times faster than ASITIC [9], an advanced algorithms based on Green's functions. Besides, only free-space Green's function is used in DBEM, which makes it capable to handle non-stratified substrates. This is verified by experiment.

References

[1] R. Gharpurey and E. Charbon, "Substrate coupling: Modeling, simulation and design perspectives," *Proc. 5th International Symposium on Quality Electronic Design*, pp. 283-290, 2004.

[2] J. P. Costa, M. Chou, and L.M. Silveira, "Efficient techniques for accurate modeling and simulation of

substrate coupling in mixed-signal IC's," *IEEE Trans. Comput. Aided Design*, vol. 18, pp. 597-607, 1999.

[3] W. Yu, Z. Wang, and J. Gu, "Fast capacitance extraction of actual 3-D VLSI interconnects using quasi-multiple medium accelerated BEM," *IEEE Trans. Microwave Theory Tech.*, vol. 51, pp. 109-199, 2003.

[4] A. M. Niknejad, R. Gharpurey, and R.G. Meyer, "Numerically stable Green function for modeling and analysis of substrate coupling in integrated circuits," *IEEE Trans. Comput. Aided Design*, vol. 17, pp. 305-315, 1998.

[5] N. K. Verghese and D.J. Allstot, "Fast simulation of substrate coupling effects in mixed-mode ICs," *IEEE Custom Integrated Circuits Conference*, pp. 18.3.1–18.3.4, 1993.

[6] T. Smedes, N.P. van der Meijs, and A.J. van Genderen, "Extraction of circuit models for substrate cross-talks," *IEEE/ACM International on Computer-Aided Design*, pp. 199-206, 1995.

[7] R. Ghapurey and R.G. Meyer, "Analysis and simulation of substrate coupling in integrated circuits," *International Journal of Circuit Theory and Application*, vol. 23, pp. 381–394, 1995.

[8] C. Xu, T. Fiez and K. Mayaram, "On the numerical stability of greens function for substrate coupling in integrated circuits," *IEEE Trans. Computer-Aided Design*, vol. 24, pp. 653–658, 2005.

[9] A. M. Nijnejad, ASITIC (Grackle Release), http://rfic.eecs. berkeley.edu/~niknejad/asitic.html.

[10] S. Donnay and G. Gielen, *Substrate Noise Coupling in Mixed-Signal ASICs*, pp.4-19, Boston: Kluwer Academic Publishers, 2003.

[11] S. Ardalan and M. Sachdev, "An overview of substrate noise reduction technieques," *Proc. 5th International Symposium on Quality Electronic Design*, pp. 291-296, 2004.

[12] X. Wang, W. Yu, and Z. Wang, "Substrate Resistance Extraction with Direct Boundary Element Method," *Asia and South Pacific Design Automation Conference*, pp.208-211, Jan. 2005.

[13] X. Wang, W. Yu, and Z. Wang, A new boundary element method for accurate modeling of lossy substrates with arbitrary doping profiles. *Asia and South Pacific Design Automation Conference*, pp. 683-688, 2006.

[14] G. H. Golub and C. F., Van Loan. *Matrix Computations*, 3rd ed. Baltimore, MD: Johns Hopkins University Press, pp.50, 1996.